

Electric Aharonov-Bohm effect without a loop in a Cooper pair box

Young-Wan Kim and Kicheon Kang*

Department of Physics, Chonnam National University, Gwangju 61186, Republic of Korea

Abstract

We predict the force-free scalar Aharonov-Bohm effect of a Cooper pair box in an electric field at a distance without forming a closed path of the interfering charges. The superposition of different charge states plays a major role in eliminating the closed loop, which is distinct from the original topological Aharonov-Bohm effect. The phase shift is determined by the charge-state-dependent local field interaction energy. In addition, our proposed setup does not require a pulse experiment for fast switching of a potential, which eliminates the major experimental obstacle for observing the ideal electric Aharonov-Bohm effect.

*Electronic address: kicheon.kang@gmail.com

I. INTRODUCTION

A charge moving in an external electromagnetic field exhibits topological quantum interference known as the Aharonov-Bohm (AB) effect [1]. An intriguing aspect of the AB effect is that the appearance of a phase shift does not require local overlap of the particle and external field. For this reason, the AB effect has been regarded as a pure topological phenomenon that cannot be described in terms of the local actions of physical variables. This property also implies that a loop geometry is essential for its observation. In the case of the electric Aharonov-Bohm (EAB) effect, interference can be observed without an overlap of the particle and the external electric field, as shown in the original work by Aharonov and Bohm [1]. The wave packet of a moving charge splits into two parts and each part propagates under different scalar potentials. The recollected wave would show interference with its phase shift proportional to the potential difference. Unlike the magnetic AB effect, a fast switching of the scalar potential is necessary to avoid overlap of the particle and the external field, which is the main technical obstacle for an observation of the ideal EAB effect. The predicted EAB effect is also topological, and is generally believed to indicate the physical significance of the (scalar) potential. The Aharonov-Casher (AC) effect [2], a related topological quantum phenomenon, describes the phase shift of a neutral particle with a magnetic moment moving around a charged rod (Fig.1 (a)). The AC effect can be regarded as the dual of the magnetic AB effect in that the roles of the charge and magnetic flux (moment) are reversed (see, e.g., Refs. 3 and 4). For the AC effect, a closed loop of the particle's path is not always required for its realization. For instance, the AC phase shift can be observed in the interference of two opposite magnetic moments of a neutral particle without dividing the particle's path (Fig. 1(b)). This "loop-free" interference had been predicted by Anandan [5] before the prediction of the topological AC effect and was experimentally demonstrated [6]. Interference can be achieved, as the AC interaction Lagrangian (and the phase accumulation) depends on the magnetic moment. Interestingly, this type of interference appears in a different context, namely, in electronic devices with Rashba spin-orbit interactions (see e.g., Refs. 7–10).

Together with the loop-free AC interference, the duality of the AB and AC effects poses an interesting question as to whether we can find an AB analogue of loop-free interference. Exchanging the roles of the magnetic moment and electric charge in the loop-free AC ef-

fect, the corresponding loop-free AB effect should appear. Basically, this is possible in a superposed state of different charges, as the AB interaction depends on the charge of the interfering particle. However, two key issues should be resolved in order to achieve loop-free AB interference. First, an ordinary charged particle cannot form a superposition of different number states, and is inappropriate for our purpose. This problem can be overcome by utilizing a superconducting condensate composed of the superposition of different numbers of Cooper pairs. The second problem is that loop-free interference cannot be described by a potential difference across two different positions (which is the case in the topological AB effect), as the test particle's wave packet would neither split nor form a closed path. Instead, the phase shift should be determined by the electrostatic energy difference (in the electric AB effect) between different charge states *at the same position*. We will show that this energy difference is described by the *geometric potential*, defined on the basis of the “Lorentz-covariant field interaction (LCFI)” approach [4, 11], whereas the magnitude of the energy difference is ambiguous in the conventional potential-based framework. A single Cooper pair box (SCB) (see, e.g., Ref. 12), composed of a superposed state of two different charges, is an ideal system for its observation. We predict a loop-free electric Aharonov-Bohm (EAB) effect in an SCB; a relative phase shift between two charge states appears in an SCB influenced by an external electric field at a distance. The magnitude of the phase shift is proportional to difference in the electrostatic energies between the two charge states. In addition, we point out that the EAB effect under the ideal condition - that the charge and external field does not overlap - can be more easily realized in this setup, as it does not require fast switching of a potential, the major technical difficulty for realizing the original force-free EAB interference in a two-path interferometer.

The paper is organized as follows. In Section II, the original EAB effect is reinvestigated in the framework of the LCFI Lagrangian, which shows that the local approach reproduces the prediction for the original topological EAB effect. Section III is devoted to our main prediction of the loop-free EAB effect for a Cooper pair box. Discussion and Conclusion are given in Sections IV and V, respectively.

II. FIELD INTERACTION APPROACH TO THE ELECTRIC AHARONOV-BOHM EFFECT.

Let us begin by briefly reviewing the original EAB effect in an ideal situation (see Fig. 2(a)) [1]. The wave packet of an incident particle with charge q splits into two parts and enter long Faraday cages. In each part, the electrical potential V_i ($i = 1, 2$) is switched on after the wave packet enters the cage. The duration of the voltage pulse should be sufficiently short to ensure that each potential is switched off far before the particle exits. The purpose of this arrangement is to avoid local overlap of the particle and electromagnetic field. Let the wave function $\psi_0(\mathbf{x}, t) = \psi_1(\mathbf{x}, t) + \psi_2(\mathbf{x}, t)$ in the absence of the potentials, where ψ_1 and ψ_2 represent the two parts. The electric potential modifies the wave function as

$$\psi(\mathbf{x}, t) = \psi_1(\mathbf{x}, t)e^{-iq \int V_1 dt/\hbar} + \psi_2(\mathbf{x}, t)e^{-iq \int V_2 dt/\hbar}, \quad (1)$$

and the interference fringe is determined by the phase difference

$$\varphi = -\frac{q}{\hbar} \int V_0 dt, \quad (2)$$

where $V_0 = V_1 - V_2$ is the potential difference.

This EAB effect can also be described in an alternative LCFI approach [4, 11]. The essence of this approach is summarized as follows. The Lagrangian governing the interaction between a charge and an external field is universally represented by the local overlap between the external field and that generated by the charge, instead of the charge being influenced by the external potential. Incorporating the Lorentz covariance and linearity in field strengths, we can uniquely determine the interaction Lagrangian:

$$L_{in} = \frac{1}{8\pi} \int F_{\mu\nu}^{(q)} F^{\mu\nu} d^3\mathbf{r}', \quad (3)$$

where $F^{\mu\nu}$ and $F_{\mu\nu}^{(q)}$ are the external electromagnetic field tensor and that generated by the charge, respectively. This Lagrangian reproduces the results derived from the potential-based approach for the classical equation of motion and the topological AB effect [4, 11]. In our arrangement of the charge with an external electric field (in the absence of an external magnetic field), the interaction Lagrangian is reduced to

$$L_{in} = -U_q = -\frac{1}{4\pi} \int \mathbf{E}_q \cdot \mathbf{E} d^3\mathbf{r}', \quad (4)$$

where U_q denotes the energy produced by the interaction between two electric fields: the external \mathbf{E} and \mathbf{E}_q produced by the moving charge.

Fig. 2(b) shows a possible configuration of the external electric field when the potentials V_1 and V_2 (of Fig. 2(a)) are switched on. The essential condition of a nonoverlapping particle and \mathbf{E} is satisfied. Nevertheless, their interaction is manifested in the overlap of \mathbf{E} with \mathbf{E}_q (not with the position of the charge) in the Lagrangian of Eq. (4). The moving charge q with speed u along the x axis generates the electric field

$$\mathbf{E}_q(\mathbf{r}) = q \frac{\gamma[(x - ut)\hat{\mathbf{x}} + y\hat{\mathbf{y}} + z\hat{\mathbf{z}}]}{[\gamma^2(x - ut)^2 + y^2 + z^2]^{3/2}}, \quad (5)$$

where $\gamma = 1/\sqrt{1 - (u/c)^2}$. For the lower path (region I), we find from Eqs. (4) and (5) that

$$L_{in} = L_{in}^I = -\frac{qV_0}{2}, \quad (6)$$

where $V_0 = \int \mathbf{E} \cdot d\mathbf{x} = V_1 - V_2$ is the potential drop across the two regions. Notably, L_{in} is independent of the speed of the moving charge. Similarly, for the upper path (region II), we obtain

$$L_{in} = L_{in}^{II} = \frac{qV_0}{2}. \quad (7)$$

Therefore, the phase difference accumulated by the interaction is

$$\varphi = \frac{1}{\hbar} \int (L_{in}^I - L_{in}^{II}) dt = -\frac{q}{\hbar} \int V_0 dt, \quad (8)$$

demonstrating that the EAB phase shift (Eq. (2)) is reproduced in the field interaction approach. Here, we have considered infinite planar conducting plates generating the potential difference, but the phase shift in Eq. (8) can be verified for an arbitrary geometry of \mathbf{E} with the potential difference V_0 across the two regions.

III. ELECTRIC AHARONOV-BOHM EFFECT IN A COOPER PAIR BOX AND THE GEOMETRIC POTENTIALS.

Next, we demonstrate how the loop-free EAB effect appears in a superposed state of different charges. An SCB [12], an artificial two-level quantum system composed of superconducting circuits, is an ideal system for realization of the loop-free EAB effect. Its quantum state $|\psi_0(t)\rangle$ is composed of a superposition of two different charge states $|q\rangle$ and $|q'\rangle$:

$$|\psi_0(t)\rangle = a(t)|q\rangle + b(t)|q'\rangle, \quad (9)$$

where $q - q' = 2e$, implying that $|q\rangle$ contains an extra Cooper pair than $|q'\rangle$. As discussed above, the charge in the SCB interacts with an external electric field (\mathbf{E}) at a distance (see the various configurations shown in Fig. 3). The quantum dynamics of an SCB is more complicated than the case of the EAB effect in a two-path interferometer. Nevertheless, it is instructive to analyze the limit of negligible charge transfer between $|q\rangle$ and $|q'\rangle$. In this limit, the quantum state evolution (modified by the distant electric field)

$$|\psi(t)\rangle \simeq a(t)e^{-iqVt/\hbar}|q\rangle + b(t)e^{-iq'Vt/\hbar}|q'\rangle \quad (10)$$

is equivalent to that of a two-path interferometer. V is the scalar potential at the position of the SCB. Switching the voltage is not required here, in contrast to the original EAB setup of moving charges. The relative phase shift is given by

$$\varphi = -\frac{(q - q')}{\hbar}Vt = -\frac{2e}{\hbar}Vt. \quad (11)$$

The problem with this result is that, unlike the original EAB phase given in Eq. (2), the phase shift of Eq. (11) remains undetermined, as V at a single position is not a quantity with a definite value.

This ambiguity is removed by adopting the LCFI Lagrangian of Eq. (4). Considering that the field interaction depends on the charge state, we can obtain a well-defined phase shift. The interaction Lagrangian for charge q and external \mathbf{E} of Eq. (4) can be rewritten in an instructive form

$$L_{in} = -U_q = -qV_G, \quad (12a)$$

where

$$V_G = \frac{1}{4\pi} \int \frac{\mathbf{E}(\mathbf{r}) \cdot \hat{\mathbf{r}}}{r^2} d^3\mathbf{r} \quad (12b)$$

is a type of scalar potential determined by the overall distribution of \mathbf{E} . This “geometric potential” (V_G) plays a similar role as an electric scalar potential but is different from the latter, as V_G at a given position is uniquely determined by the distribution of \mathbf{E} . Therefore, the charge-state-dependent phase shift is also uniquely determined. From Eq. (12) we obtain the state evolution

$$|\psi(t)\rangle \simeq a(t)e^{-iqV_Gt/\hbar}|q\rangle + b(t)e^{-iq'V_Gt/\hbar}|q'\rangle \quad (13)$$

and the well-defined relative phase shift

$$\varphi = -\frac{2e}{\hbar}V_Gt. \quad (14)$$

This constitutes the EAB effect in an SCB without forming a loop of the particle's path.

As the EAB phase shift is entirely determined by V_G , it will be useful to evaluate its values for different cases (see Fig. 3). First, consider a capacitor composed of a pair of two infinite parallel conducting plates (Fig. 3(a)). The field interaction energy is equivalent to that obtained in Eq. (6), and we find that

$$V_G = \frac{V_0}{2}, \quad (15)$$

where V_0 is the voltage drop across the two plates. Similarly, in the presence of two such parallel capacitors (Fig. 3(b)),

$$V_G = (V_0 + V'_0)/2 \quad (16)$$

for the two voltage drops V_0 and V'_0 (measured from the SCB position) across the upper and lower capacitors, respectively.

In fact, V_G can be evaluated for a capacitor with an arbitrary shape (Fig. 3(c)). The external field can be written as $\mathbf{E} = E_0\hat{\mathbf{n}}$, where $\hat{\mathbf{n}}$ is the unit vector perpendicular to the capacitor surface, and Eq. (12b) is reduced to

$$V_G = \frac{1}{4\pi} \int E_0\hat{\mathbf{n}} \cdot \hat{\mathbf{r}} dr d\Omega. \quad (17a)$$

By noting that the potential drop across the capacitor can be expressed as

$$V_0 = \int E_0\hat{\mathbf{n}} \cdot \hat{\mathbf{r}} dr, \quad (17b)$$

we obtain the relation

$$V_G = \frac{\Omega}{4\pi} V_0, \quad (17c)$$

where Ω is the solid angle formed by the capacitor geometry. In all cases of Fig. 3, the EAB phase shift in Eq. (14) is determined by the geometry-dependent potential V_G and not by the voltage difference V_0 . This result is in contrast with the original EAB effect where only the voltage difference of two interfering paths matters.

The EAB effect discussed above can be demonstrated in a realistic SCB circuit (see Fig. 4). An experimental SCB circuit is controlled by the gate voltage V_g . The circuit has two capacitances, the junction capacitance C_J and gate capacitance C_g . A new component here is the inclusion of the geometric potential (V_G) associated with the electric field that is spatially separated from the circuit.

The electrostatic energy of this system has the form

$$\frac{C_J}{2}V_J^2 + \frac{C_g}{2}(V_g - V_J)^2 + qV_G, \quad (18)$$

where V_J is the voltage across the tunnel junction. Josephson coupling leads the relation between the phase variable (ϕ) and V_J : $\dot{\phi} = 2eV_J/\hbar$. The island charge is $q = C_JV_J - C_g(V_g - V_J) = C_\Sigma V_J - C_gV_g$, where $C_\Sigma = C_J + C_g$ is the total capacitance. Including Josephson coupling (with the constant E_J) as well, the Lagrangian of the system is given by (omitting constant terms)

$$L(\phi, \dot{\phi}) = \frac{C_\Sigma}{2} \left[\frac{\hbar}{2e} \dot{\phi} - \frac{1}{C_\Sigma} (C_g V_g - C_\Sigma V_G) \right]^2 + E_J \cos \phi. \quad (19)$$

Adopting the standard procedure of the Legendre transformation, we obtain the Hamiltonian

$$H = E_c(\hat{n} - n_G - n_g)^2 - E_J \cos \phi, \quad (20)$$

where $E_c = (2e)^2/2C_\Sigma$ is the charging energy of a single Cooper pair. The number of excess Cooper pairs (\hat{n}) of the island satisfies the commutation rule $[\phi, \hat{n}] = i$ and is limited to $\hat{n} = 0, 1$ in an SCB. The effects of the geometric and gate voltages are included in the variables $n_G = C_\Sigma V_G/2e$ and $n_g = -C_g V_g/2e$, respectively.

The eigenvalues of this Hamiltonian are

$$E_\pm = \mp \frac{1}{2} \sqrt{[E_c(1 - 2n_g) - 2eV_G]^2 + E_J^2}; \quad (21a)$$

therefore, the evolution of the quantum state depends on V_G . Fig. 5 displays the qubit spectra both with and without the geometric potential. The spectrum is shifted in the presence of the geometric potential (V_G), and this is the result of the interaction of the qubit charge with the electric field at a distance (as described in Eq. (12)). Accordingly, the transition frequency

$$\omega = \frac{1}{\hbar}(E_- - E_+) = \frac{1}{\hbar} \sqrt{[E_c(1 - 2n_g) - 2eV_G]^2 + E_J^2} \quad (21b)$$

also depends on V_G . The EAB effect manifested in Eq. (21) can be probed in the standard SCB circuit [12, 13]. The only new component here is to incorporate an external electric field spatially separated from the circuit. The effect will become prominent when $2eV_G$ becomes comparable to E_c . Typical value of charging energy is $E_c \sim 100\mu\text{eV}$ [14, 15], and therefore a variation of the voltage drop $0 \leq V_0 \lesssim 100\mu\text{V}$ (e.g., between the conducting

plates in Fig. 3(a)) would be ideal for observation of the EAB effect. As the measurement techniques in the superconducting qubits are well established both in the energy- and the time-domain experiments (see e.g., Refs. 12, 13), exploring the EAB effect of Eq. (21) is possible with the standard measurement scheme. For example, measurement of the qubit state can be implemented by connecting the SCB to an electrometer composed of a single electron transistor (SET) (see Fig. 6). The state readout can be performed by measuring the qubit-state-dependent current through the SET [13].

IV. DISCUSSION.

Let us discuss several notable aspects of our results. First, the loop-free EAB effect in an SCB cannot be properly accounted for by the conventional scalar potential, as the latter does not provide a definite value at a given position (see Eq. (11)). The effect is instead described by the geometric potential V_G (Eq. (12b)), which is determined by the geometry of the external field distribution and not simply by the potential difference between different positions. In other words, the EAB effect in our arrangement is understood only by specifying the local overlap of the external field and the field generated by the interfering charge (Eq. (4)), demonstrating the locality of the interactions.

Second, consider charge redistribution on the conducting plate induced by the SCB charge q (Fig. 7). This may influence the interaction between \mathbf{E}_q and \mathbf{E} , and its consequences should be clarified. For simplicity, the conductor is assumed to be ideal; the charges on its surface are free to move in response to q . A naive expectation would be that the field \mathbf{E}_q generated by q is compensated by the field \mathbf{E}_i generated by the induced charges; $\mathbf{E}_i + \mathbf{E}_q = 0$. If this is the case, the interaction between \mathbf{E}_q and the external field \mathbf{E} would be completely removed. This would result in the disappearance of the EAB effect in the SCB.

However, this naive expectation is incorrect, as the quantum nature of \mathbf{E}_i is not taken into account. In a quantum mechanical treatment, only the expectation value of $\mathbf{E}_i + \mathbf{E}_q$ vanishes, whereas the interaction between q and the external field is not shielded at all, as we show below (see also Ref. 4). The charged particles in the conductor contribute to the field interaction Lagrangian as

$$L'_{in} = - \sum_j q_j V_G(\mathbf{r}_j), \quad (22)$$

where q_j and $V_G(\mathbf{r}_j)$ are the charge and geometric potential (defined as Eq. (12b)) at position \mathbf{r}_j on the conductor. For a capacitor with an arbitrary shape (Fig. 3(c)), the geometric potential (Eq. (17c)) depends only on the solid angle formed by the capacitor and is independent of \mathbf{r}_j . Therefore, the interaction Lagrangian $L'_{in} = -(\sum_j q_j)V_G$ is independent of the redistribution of the particles in the conductor, implying that charge redistribution does not affect the interactions between \mathbf{E}_q and \mathbf{E} at all. The EAB interference is unaffected by the induced charges of the conductor. We can equally apply this argument to the original topological EAB effect. In addition, the interaction between \mathbf{E}_q and \mathbf{E}_i also does not affect the EAB effect, as it is independent of \mathbf{E} .

Third, although our study is focused on the simpler EAB effect, it is also possible to demonstrate a magnetic AB effect without a loop. Moving particles with superposed charge states are necessary to achieve it. This can be realized, for example, by utilizing the Andreev reflections in superconductor-metal hybrid junctions [16].

Finally, note that the EAB experiment of the original form (as in Fig. 2(a)) has never been performed. This is primarily because its realization would require extremely fast switching of the electric potential at one of the Faraday cages placed along the path of the charged particle (see, e.g., Ref. 17). This technical difficulty does not exist in our SCB analogue. The interference of the two different charge states instead of two spatially separated paths is manifested in the qubit's interaction with a static external field at a distance. The elimination of the requirement of fast switching of the electric potential would enable much easier realization of the ideal force-free EAB effect.

V. CONCLUSION.

In conclusion, we have predicted the scalar AB effect without a loop in a Cooper pair box interacting with an external electric field at a distance. The superposition of different charge states eliminates the requirement of loop geometry for the interferometer. The phase shift is given by the charge-state dependence of the field interaction energy and is universally represented by the geometric potential. Our proposal provides an easy way to realize the ideal EAB effect, as the setup does not require a pulse experiment for fast switching of the

potential, which has been the major technical obstacle for its observation.

- [1] Y. Aharonov and D. Bohm, *Phys. Rev.* **115**, 485 (1959).
- [2] Y. Aharonov and A. Casher, *Phys. Rev. Lett.* **53**, 319 (1984).
- [3] B. Reznik and Y. Aharonov, *Phys. Rev. D* **40**, 4178 (1989).
- [4] K. Kang, *Phys. Rev. A* **91**, 052116 (2015).
- [5] J. Anandan, *Phys. Rev. Lett.* **48**, 1660 (1982).
- [6] K. Sangster, E. Hinds, S. M. Barnett, and E. Riis, *Phys. Rev. Lett.* **71**, 3641 (1993).
- [7] S. Datta and B. Das, *Appl. Phys. Lett.* **56**, 665 (1990).
- [8] R. I. Shekhter, O. Entin-Wohlman, M. Jonson, and A. Aharony, *Phys. Rev. Lett.* **116**, 217001 (2016).
- [9] D. Tomaszewski, P. Busz, R. López, M. Lee, J. Martinek, et al., *Phys. Rev. B* **97**, 214506 (2018).
- [10] A. Aharony, O. Entin-Wohlman, M. Jonson, and R. Shekhter, *Phys. Rev. B* **97**, 220404 (2018).
- [11] K. Kang, arXiv:1308.2093 (2013).
- [12] Y. Makhlin, G. Schön, and A. Shnirman, *Rev. Mod. Phys.* **73**, 357 (2001).
- [13] G. Wendin and V. Shumeiko, *Low Temp. Phys.* **33**, 724 (2007).
- [14] Y. Nakamura, Y. A. Pashkin, and J. Tsai, *Nature* **398**, 786 (1999).
- [15] O. Astafiev, Y. A. Pashkin, Y. Nakamura, T. Yamamoto, and J.-S. Tsai, *Phys. Rev. Lett.* **93**, 267007 (2004).
- [16] K. Kang, *J. Korean Phys. Soc.* **71**, 565 (2017).
- [17] H. Batelaan and A. Tonomura, *Phys. Today* **62**, 38 (2009).

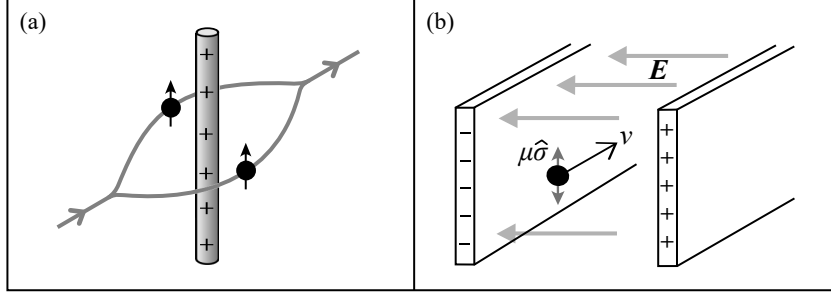


FIG. 1: Illustration of (a) the topological Aharonov-Casher effect of a neutral particle with a fixed magnetic moment, and (b) the loop-free analog of the Aharonov-Casher interference of a superposed spin.

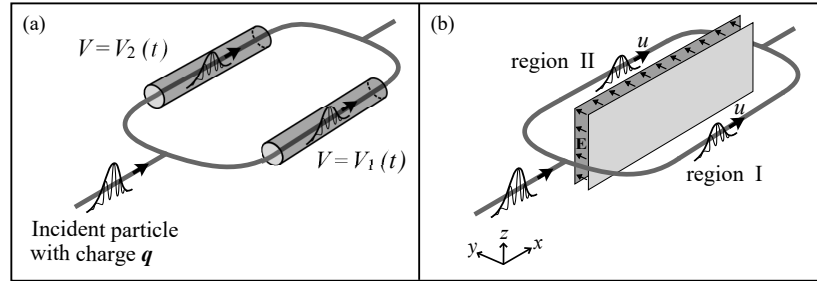


FIG. 2: An ideal setup of the force-free electric Aharonov-Bohm effect: (a) the original arrangement of Aharonov and Bohm [1] and (b) an equivalent situation with the potential difference represented by the electric field localized between two paths.

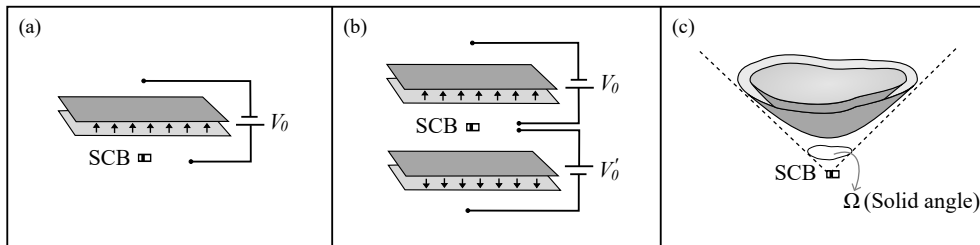


FIG. 3: Various configurations of the electric field at a distance from the location of the Cooper pair box. The electric Aharonov-Bohm effect can be tested with these arrangements, each of which yields a different geometric potential: (a) $V_G = V_0/2$, (b) $V_G = (V_0 + V'_0)/2$, and (c) $V_G = V_0\Omega/4\pi$, where Ω is the solid angle formed in the configuration of the external field.

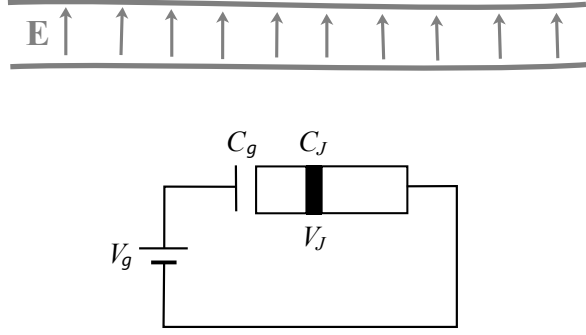


FIG. 4: A single Cooper pair box (SCB) circuit in the presence of an arbitrary distribution of the external electric field spatially separated from the circuit. The setup is equivalent to the standard SCB circuit, except that the distant electric field distribution gives rise to an additional field interaction energy.

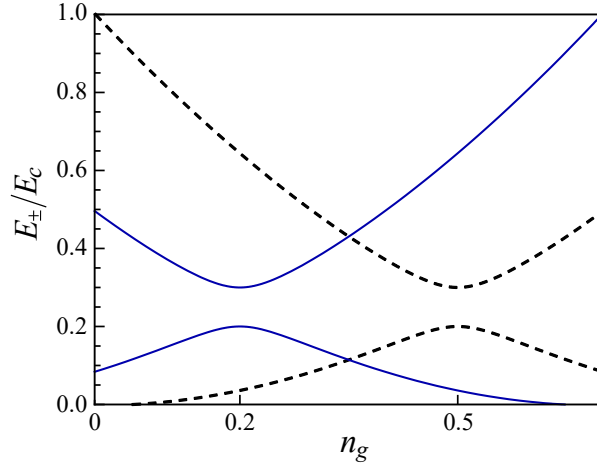


FIG. 5: Electric Aharonov-Bohm effect in the spectrum of an SCB. Solid (Dashed) lines represent the gate dependence of the qubit eigenstate energies for $2eV_G/E_C = 0.6$ ($2eV_G = 0$) and $E_J/E_C = 0.1$. The shift of the spectrum at nonzero V_G results from the interaction of the SCB charge with the external electric field at a distance.

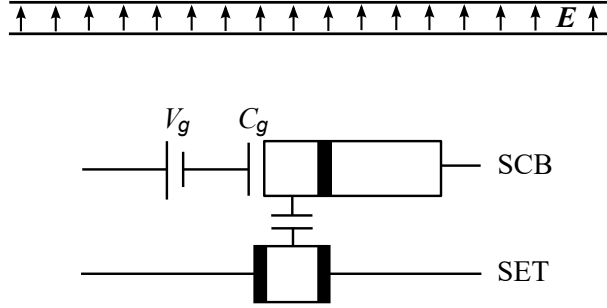


FIG. 6: A possible measurement scheme of the qubit state with a single electron transistor capacitively coupled to the SCB. This measurement can probe the electric Aharonov-Bohm effect manifested in the qubit state.

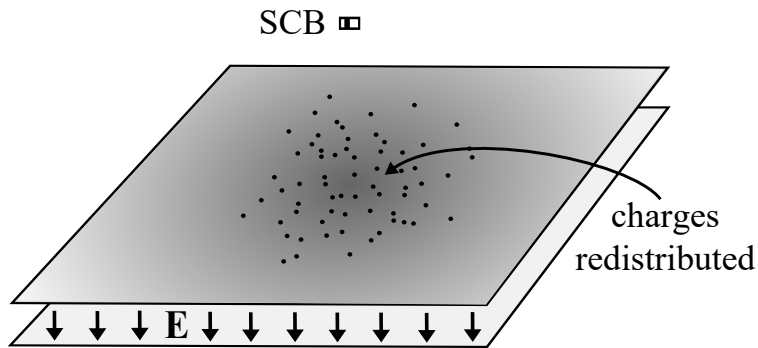


FIG. 7: Illustration of the charge redistribution on the surface of the conducting plate induced by the SCB charge q .